MEASURING PRESENT-DAY STRAIN RATES ALONG THE FISH LAKE VALLEY FAULT SYSTEM, PACIFIC-NORTH AMERICA PLATE BOUNDARY

A Thesis
Presented to
The Academic Faculty

by

Christopher William Johnson

In Partial Fulfillment
of the Requirements for the Degree
B.S. Earth and Atmospheric Science with Research Option in the
School of Earth of Atmospheric Science

Georgia Institute of Technology
May 4th, 2012

MEASURING PRESENT-DAY STRAIN RATES ALONG THE FISH LAKE VALLEY FAULT SYSTEM, PACIFIC-NORTH AMERICA PLATE BOUNDARY

Approved by:

Dr. Andrew V. Newman, Advisor
School of Earth and Atmospheric Science
Georgia Institute of Technology

Dr. Josef Dufek
School of Earth and Atmospheric Science
Georgia Institute of Technology

Dr. Dana Hartley
School of Earth and Atmospheric Science
Georgia Institute of Technology

Date Approved: May 4th, 2012

I would like to dedicate the following research project to Dr. Kurt Frankel. I began working with Kurt and his research group in May 2010 on a project in the Eastern California shear zone. On July 2, 2011, after completing the second field season, Kurt's life was tragically taken in an automobile accident. I would like to thank Kurt for his shared knowledge, support, and advice while working together. Kurt's passion for science was inspirational to everyone he encountered and he will not be forgotten.

ACKNOWLEDGEMENTS

First I would like to thank my advisors on this project, Kurt Frankel and Andrew Newman. They both uniquely enhanced my learning experience at Georgia Tech. I would also like to thank Andrew Newman and Josef Dufek for suggestions and improvements to this manuscript. I extend my gratitude to Zach Lifton for his help and advice while collecting and processing data. This project was financially supported by NSF, Geological Society of America, Georgia Tech UROP, and Georgia Tech Rutt Bridges.

TABLE OF CONTENTS

LIST OF TABLES

LIST OF FIGURES

LIST OF SYMBOLS AND ABBREVIATIONS

º	degree
b	far field velocity
D	fault locking depth
DVFLV	Death Valley – Fish Lake Valley
E	East
ECSZ	Eastern California shear zone
FLV	Fish Lake Valley
GPS	Global Positioning System
GT	Georgia Institute of Technology
km	kilometer
M7.0	magnitude 7.0
m	meter
Ma	million years (Mega anna)
mm	millimeter
NGS	National Geodetic Survey
Π	pi
SAF	San Andrea fault
W	West
UNR	University of Nevada, Reno
V	modeled velocity
X	fault normal distance
yr	year

SUMMARY

The eastern California shear zone (ECSZ) is located east of the San Andreas fault and contains a complex network of structures that accommodate ~25% of the relative displacement between the Pacific and North American plates. Geodetic data indicate strain accumulation at a rate of 12±2 mm/yr along four main structures in the ECSZ. The Death Valley-Fish Lake Valley fault, the prominent and longest fault in the ECSZ at ~300km, is observed to be the fastest slipping fault in the region storing elastic strain at a rate of 3-8 mm/yr. Recently determined long-term slip rates (10^3 – 10^6 year timescale) indicate a pattern of decreasing velocity moving north through Fish Lake Valley (FLV) from ~6 mm/yr to zero, presumably because strain is transferred onto extensional faults located to the east. This study intends to determine the short-term (decadal timescale) displacement field along the FLV fault using Global Positioning System (GPS) derived velocities to test whether spatial patterns of geodetic and geologic rates are consistent through time. In a series of two GPS campaigns in 2010 and 2011, nine geodetic monuments, spaced 15-20 km apart, were surveyed in and around FLV. In addition, campaign data from previous surveys has been acquired from UNAVCO. The combined data sets are used to calculate the relative motion along the fault. Modern strain rates determined using an elastic half space model resulted in a slip rate of ~3.8 mm/yr across the FLV fault. This rate is examined with respect to previously determined Quaternary rates along the FLV fault.

CHAPTER 1

INTRODUCTION

A fundamental issue in modern tectonics is the degree to which spatial and temporal variations in strain accumulation and release exist along evolving plate boundaries. An earthquake is a release mechanism for the elastic strain accumulated within the crust between seismic events. Recurrence intervals of earthquakes are dependent on the rate of strain accumulation within the primary fault system and surrounding subsidiary faults. Located in California, the San Andreas fault (SAF) is the major feature of the Pacific-North America plate boundary that extends from the Gulf of California to San Francisco and into the Pacific Ocean with multiple associated subsidiary faults. Research concerning subsidiary fault systems increases the understanding of the plate boundary evolution, the distribution of plate tectonic strain through Earth's crust, and the reliability of natural hazard assessment in tectonically active regions. Recurrence intervals of large earthquakes are estimated using strain rates associated with motion along a fault system; accurately determining the rate of strain accumulation results in more precise earthquake recurrence interval predictions along with an improved understanding of the dynamics and evolution of fault systems. In modern history, major cities located near this fault system experienced significant damage due to large (>M7.0) earthquakes. This study aims to enhance the understanding of one fault contained in the complex network of subsidiary faulting east of the plate boundary.

The western United States is a unique region of the world that contains a transform plate boundary within the continental crust. Along this boundary the Pacific and North American plates slide ~50 mm/yr relative to one another with ~38 mm/yr accommodated by the SAF and ~25% of the displacement on subsidiary faults in the

region east of the Sierra Nevada (Bennett et al., 2003; Hammond and Thatcher, 2007; Frankel et al., 2011). Areas of subsidiary faulting along the Pacific-North American plate boundary include the eastern California shear zone (ECSZ), Walker Lane, and the Basin and Range. The application of Global Positioning System (GPS) to geodetic studies provides high precision displacement rates (~1 mm/yr) that are used to infer the short-term strain rates throughout these regions of complex and diffuse faulting. Previous research shows a temporal and spatial variation exists between long-term ($10^3 – 10^6$ year) and short-term (decadal) rates of deformation in regions of complex faulting (Reheis and Sawyer, 1997; Friedrich et al., 2003; Frankel el al., 2007; Oskin et al., 2007; Frankel et al., 2011). This discrepancy in strain accumulation is not well understood. Possible explanations include a variation in strain accumulation over time due to plate tectonic driving forces in a system, strain transfer between faults in the region, or as yet unidentified faults accommodating strain. Accurately describing the distribution of strain along plate boundaries is one of the keys to understanding the evolution of a plate boundary. This review of literature describes the research that considers the transfer of strain onto additional structures.

Accounting for total strain in a system is important in understanding the dynamics of strain transfer. The Death-Valley Fish Lake Valley (DVFLV) fault is the longest and most active subsidiary fault along the plate boundary. This structure traverses from Death Valley in eastern California northwards for ~300 km into western Nevada. Dixon et al. (2000) conducted the first GPS study in the southern Walker Lane, and the resulting geodetic models suggest the Sierra Nevada acts as a rigid block rotating counter-clockwise with respect to North America. Dextral motion between the Sierra Nevada and southern Walker Lane is transferred onto two faults situated at ~37.5ºN, Owens Valley fault and Fish Lake Valley (FLV) fault, and separated by the White Mountains (Dixon et al., 2000, 2003; Oldow, 2003; Wesnousky, 2005a). Bounding the White Mountain block to the north and south are a series of down-to-the-northwest normal faults. Studies

indicate these normal faults transfer strain from Owens Valley to FLV, thereby increasing the strain rate to the north on the FLV fault (Reheis and Dixon, 1996; Lee et al., 2001, 2009). Dextral shear at this latitude, determined from GPS, indicate a region-wide strain rate of 9.3±0.2 mm/yr and presumably FLV fault stores ~90% of the strain transfer (8.2±2.0 mm/yr) to the southern Walker Lane (Dixon et al., 2000; Bennett, 2003). Modern strain rates and presumed strain transfer contradict geologic rates of deformation. Paleoseismic studies in the ECSZ and southern Walker Lane indicate strain rates equaling half the observed modern values in FLV.

Previously determined paleoseismic slip rate measurements along the DVFLV fault indicate a pattern of temporal variation in the Miocene through the Quaternary (Reheis and Sawyer, 1997; Frankel, 2007; Ganev, 2010; Frankel, 2011). Stratigraphy and chronology mapping by Reheis and Sawyer (1997) for the Miocene and Pleistocene indicate lateral motion on the fault began ~10 Ma, which coincides with the onset of Basin and Range right-lateral shear. Slip rates were seen to vary according to epoch markers used for each location on the fault. Long-term dextral slip rates from ~10 Ma average ~5 mm/yr with a substantial increase to 11 mm/yr during the middle Pleistocene and late Pleistocene only to return to 4 mm/yr during the onset of extensional faulting ~5 Ma (Reheis and Sawyer, 1997). Consistent in measurements from each epoch, Reheis and Sawyer (1997) conclude slip rates decrease from Oasis to Chiatavich Creek, 4-5 mm/yr to 1-2 mm/yr respectively, from the Miocene to the Pleistocene. Frankel et al. (2011) concluded late Quaternary along strike slip rates follow a similar trend, decreasing from ~6 mm/yr in southern FLV between Cucomongo Canyon and Oasis to 0 mm/yr moving north. The geographic rate change is presumably a result of strain transfer off the FLV fault onto diffuse extensional faulting to the northeast with the eastward propagation beginning at Leidy Creek (Reheis and Sawyer, 1997; Frankel et al., 2011). Investigating the transfer of strain, Ganev et al. (2010) found geologic evidence for a northeastward transfer of strain off FLV fault and into the Mina Deflection, a region of complex normal

and sinistral faulting. Hoeft and Frankel (2010) and Foy (2011) concluded the Silver Peak-Lone Mountain extensional complex to the east accommodates a portion of the missing strain in a diffuse complex of normal faults with the possibility of multiple structures not expressed on the surface accumulating the strain deficit. Neither study conclusively locates the missing strain from the FLV fault but each provides evidence for additional investigation in FLV to reconcile the spatial variation in strain transfer. A comparison of modern strain rates on individual faults will determine if constancy exists from the Holocene through the late Pleistocene. Short-term displacement rates are needed to show if the strain accumulation observed in the long-term geologic record appears in present-day rates of strain accumulation.

The project builds upon a GPS campaign in the southern Walker Lane and ECSZ as part of ongoing research in the region to monitor surface deformation. Using GPS, I measured slip rates in and around Fish Lake Valley, NV, analyzed the strain accumulation in the system, and compared patterns observed from previously determined long-term geologic rates. I hypothesize that if strain rates are constant in time then GPS data should indicate a northward decreasing rate of strain accumulation along the FLV fault as strain in the system is transferred eastward. However, if short-term rates of strain accumulation along the FLV fault do not match long-term rates, this implies a temporal variation in strain accumulation and release, which has important implications for understanding the earthquake cycle.

CHAPTER 2

METHODS

2.1 Study Area

The ECSZ and Walker lane are characterized by transient shear along discontinuous faults as strain is presumably transferred from the rigid Sierra Nevada into the Basin and Range (Dixon et al., 2000, 2003; Oldow, 2003; Wesnousky, 2005a). The FLV fault is located on the range front of the White Mountains in Fish Lake Valley, NV along the California-Nevada border. FLV is ~80 km trending NNW and ~25 km wide in the north and ~8 km wide in the south (Figure 1). The southern boundary is defined by the intersection of Deep Springs fault with FLV as normal faulting structurally connects the Owens Valley fault to the east (Lee et al., 2001). North of the White Mountains is a region of E-W trending, left-lateral strike slip faulting, referred to as the Mina deflection, which structurally connects the Sierra Nevada to the Basin and Range (Oldow et al., 1994, 2001; Wesnousky, 2005b; Lee et al., 2009). The complexities of the Mina deflection are not addressed in this study; of interest is the transfer of strain from the FLV fault onto the Mina deflection via the Silver Peak-Lone Mountain range. Shown in black are Quaternary slip rates (mm/yr) determined by Frankel et al. (2011) that indicate a transfer of strain beginning at ~37.5˚ N and decrease moving north, suggesting strain is transferred east into the Mina deflection, not down the Fish Lake Valley fault.

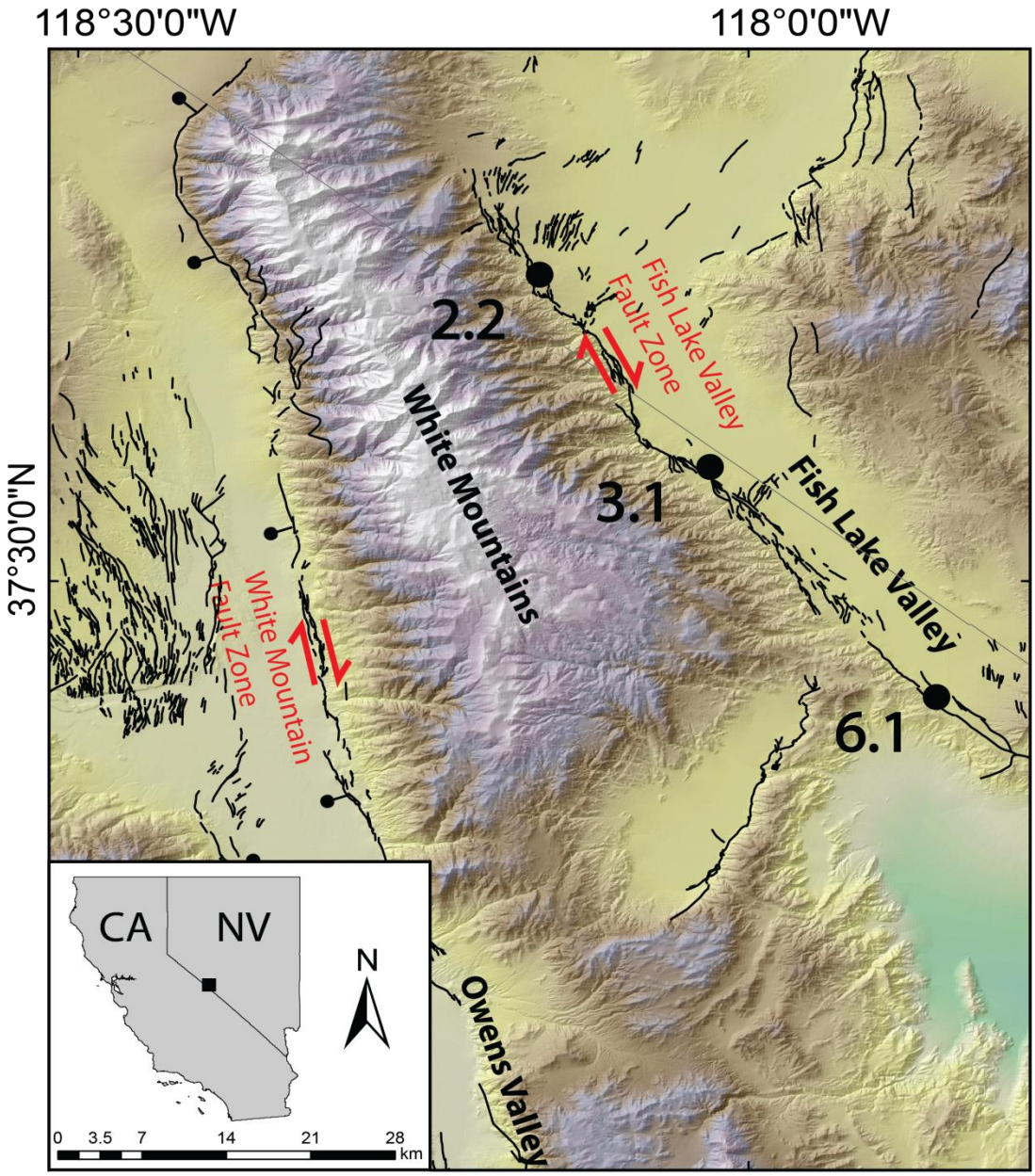

Figure 1: The White Mountains are bounded by the Owens Valley fault and Fish Lake Valley fault. Shown in black are Quaternary slip rates (mm/yr) determined by Frankel et al. (2011).

2.2 Data Collection

Interseismic displacement across active faults is obtained using high precision GPS. The southern Walker Lane contains an increasingly dense network of GPS survey

monuments that continues to expand with ongoing research efforts. Survey locations include permanent GPS receivers and multiple campaign sites with data archived and accessible at UNAVCO. Survey locations in this study were established by Georgia Institute of Technology (GT), United States National Geodetic Survey (NGS), and PIs conducting geodetic research throughout the region, namely PIs at the University of Nevada-Reno (UNR). The use of non-GT survey locations is necessary to establish a time series for relative displacement at each location. GT sites established in 2010 will not provide useable results until the completion of three campaigns. UNR and NGS survey sites were established before 2005. Reoccupying older survey locations provide time series >6 years in many locations but result in a variable resolution throughout the velocity field.

The survey sites are separated by ~15 km and require a clear line-of-sight above 11º elevation to receive the maximum number of satellite signals. A typical location is above the valley floor on a ridge containing exposed bedrock. Monuments installed by GT consist of a 16 x 200 mm non-corrosive steel pin permanently secured into bedrock with epoxy to ensure displacement is the result of ground motion (Figure 2). Monuments installed by NGS are flush markers installed in a concrete footing. Monuments installed by PIs at UNR utilize a steel rod designed to accept a quick-connect coupling mount. Additional pins in the area are flush with the bedrock, similar to NGS. All pins, except the UNR locations, contain a dimple recess for positioning the tripod antenna mount to ensure a consistent installation during each occupation.

Figure 2: GPS equipment and survey monument.

Monitoring the survey locations is completed with a Zephyr Geodetic antenna and Trimble R7 receiver represented in Figure 2. A recording time of 72 hours with a 15 second sample rate (0.066 Hz) is required for each location. A 72 hour time span increases the precision of the signal and reduces error in velocity calculation. The antenna is installed using a spike mount tripod designed and built at GT. The antenna is secured to a spike 0.5 m above the survey pin and positioned vertical with two <0.5 mm precision levels. With three independently locked legs the design is stable in most weather conditions. All level positions are measured and recorded before and after survey occupation to ensure no movement of the spike mount occurred. Survey locations maintained by GT are reoccupied each year using the same antenna, receiver, and spike

mount to ensure consistency in the data set. Survey locations installed and maintained by UNR require a quick-connect adapter to secure the antenna to the monument. The height difference in the antenna mount is notated and required for processing calculations. Accurate records and proper installation is critical to resolve the ~0 - 2 mm/yr displacement expected throughout the study area.

2.3 Data Procssing

All data is processed using GIPSY software at the University of Miami. Already existing data sets acquired from UNAVCO are reprocessed with new GPS positions to ensure consistent analysis of older data sets. GPS positional estimates are determined for each epoch, or the satellites position and time recorded at 0.066 Hz. A positional estimate is averaged for a daily solution. The resulting RINEX files contain a displacement for each daily solution at the corresponding survey monument relative to permanent land bases locations calibrated for GPS processing. The reference frame of the displacement desired in this study contains a stable North America and is determined using the NA-ITRF2005 orbital reference. All calculations are performed in MATLAB and result in three-dimensional point positions and a time-series velocity for each survey monument relative to North America. A regional velocity field is resolved through these position vectors.

2.4 Displacement Model

A screw dislocation model is used to determine the best-fit far field velocity and locking depth using survey locations that form a transect across the fault plane (Savage and Burford, 1973). Solutions are calculated for each survey location using the interseismic strain relation that considers elastic deformation decreasing with distance

from the fault plane. $V = b / \pi * \text{atan}(X / D)$, V is the modeled velocity, b is the far field velocity, X is the orthogonal distance to b, D is the fault locking depth. The model assumes an infinitely long fault thus negating the fault normal component of displacement and utilizing the parallel component only. This assumption is appropriate for the modeling style and considering the strike-slip nature of the FLV fault. Coordinates are converted to a Cartesian coordinate system centered on the FLV fault at 37.682200, -118.104118. From this location the fault plane and all velocities, components, and errors are rotated clockwise 31.0º to align the fault plane with north.

Solutions are determined for each survey monument location by iterative calculations through a range of far field velocity and fault locking depth of -10.0-10.0 mm/yr and 0.0-50.0 km, respectively. A velocity normalizing factor is determined during each calculation considering the two free variables, b and D, to eliminate the regional motion incorporated into the velocity component during all statistical calculations. A best fit solution is determined from a grid search of the reduced Chi Square values comparing the variance of the modeled velocity and normalized velocity. All calculations are performed using MATLAB software, and data results are represented using GMT software.

CHAPTER 3

RESULTS

3.1 GPS Survey

Nine survey locations with a range of ~60 km were selected to model the displacement across the fault. GPS results are displayed in Figure 3 and include the north and east component of displacement relative to NA-ITRF-2005 starting at the initial survey date. Daily positional estimates are combined to represent a time series for each location. Annual campaign locations result in 3-20 solutions per year. Continuous locations, DYER and P652, result in daily solutions for the duration of deployment. A least squares regression analysis between the initial and final survey period represents the displacement rate in mm/yr. The vertical displacement is disregarded for this study as the model only considers strike-slip faulting without a normal component. Figure 4 represents resolved velocity vectors with 95% confidence error ellipses selected to describe an approximate orthogonal transect across the FLV fault. All survey monuments coordinates and associated displacement rates are listed in Table 1. The north and east covariance is also listed and used in calculating the coordinate transformation necessary for the dislocation model.

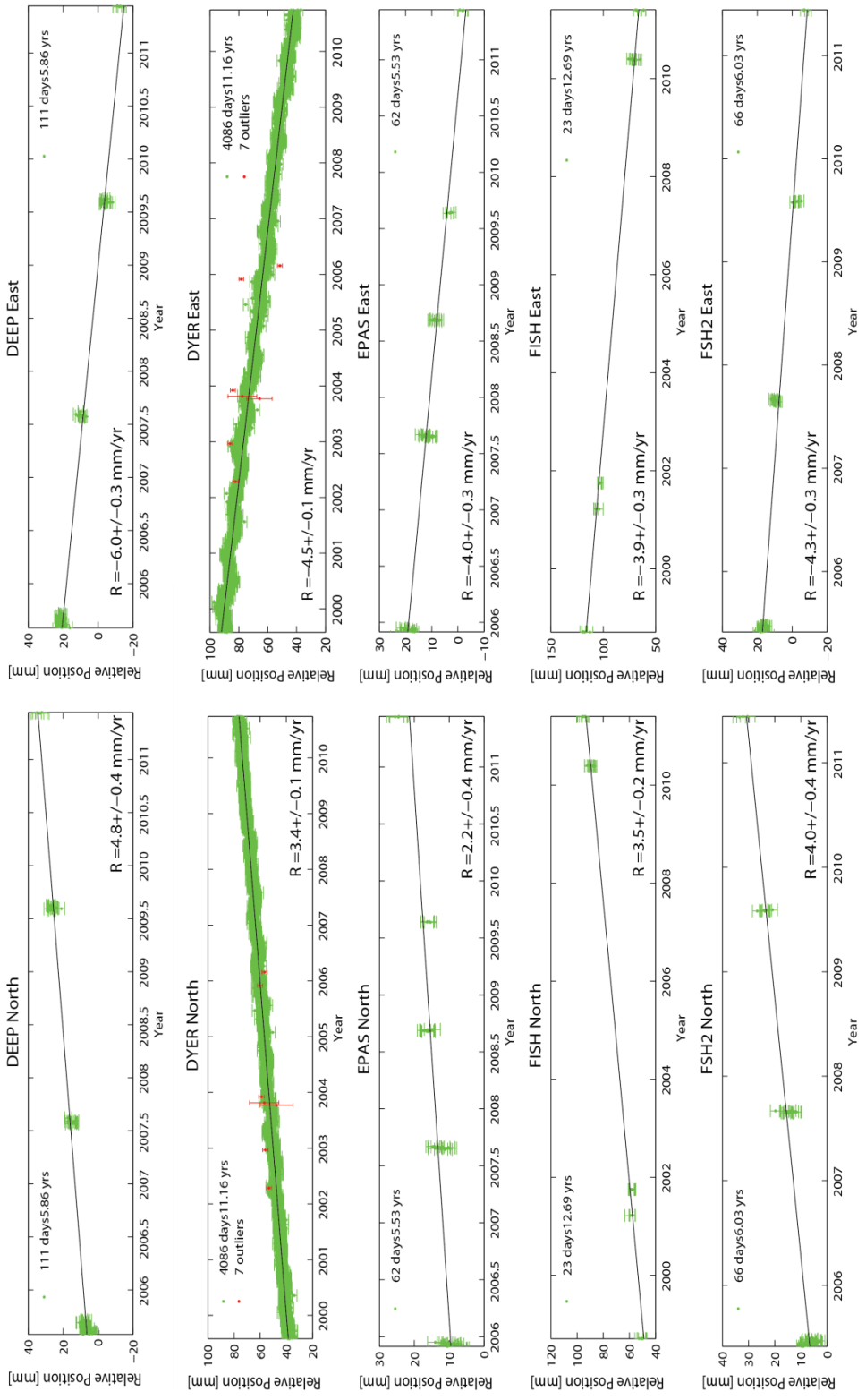

Figure 3: Displacement rates for the nine survey locations selected to represent the study area.

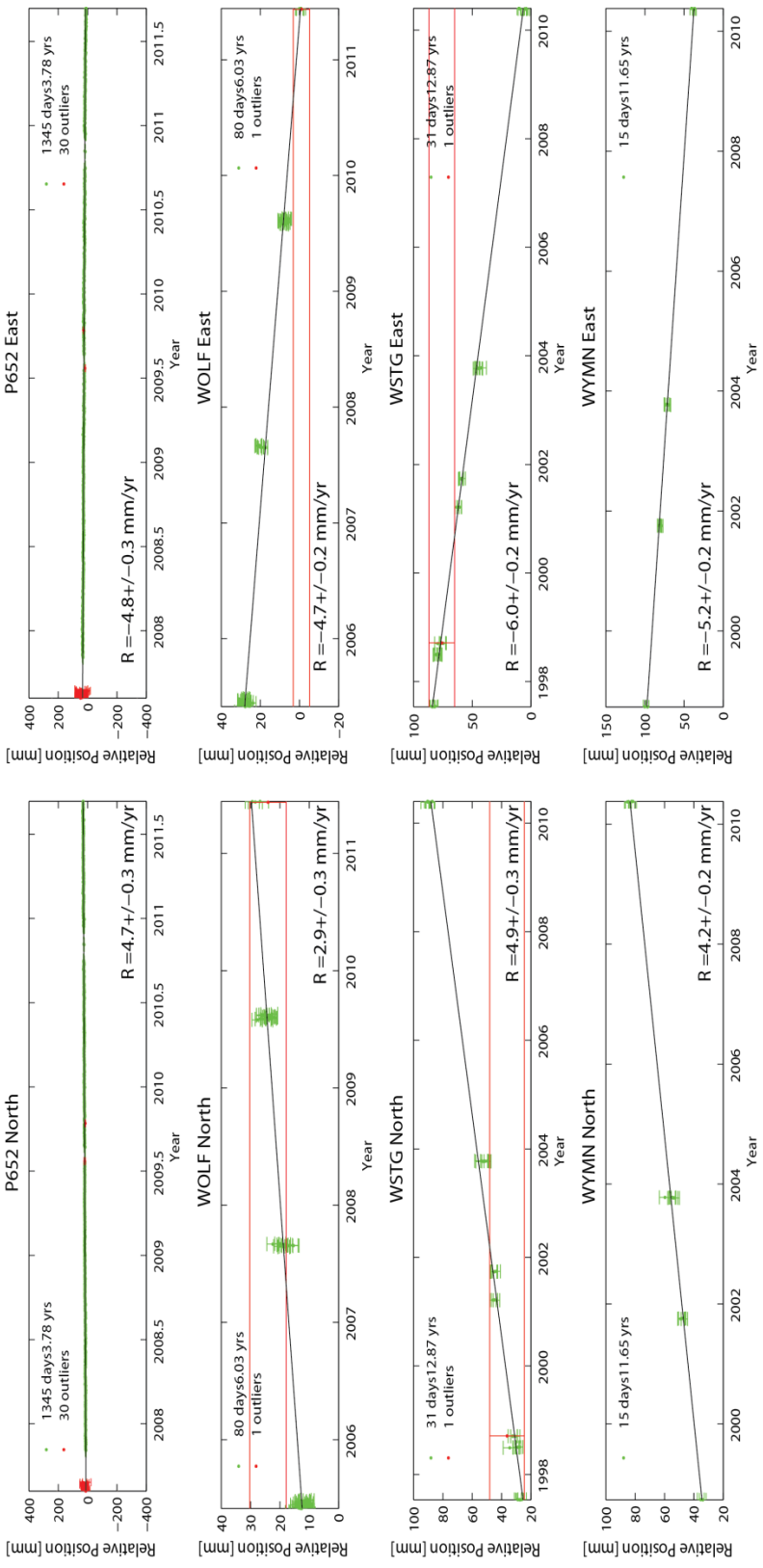

Figure 3: continued.

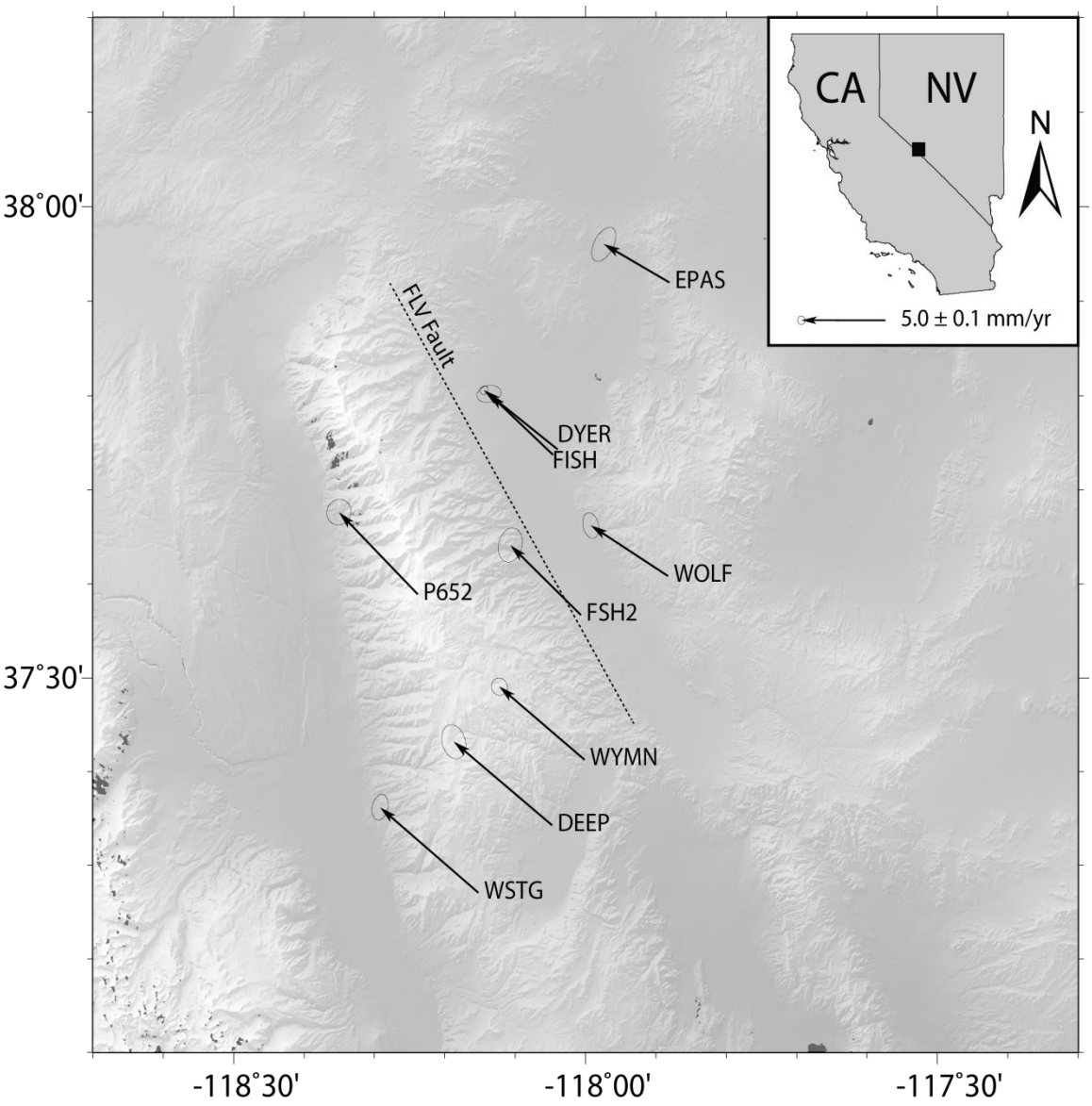

Figure 4: Resolved velocity vectors with 95 % confidence error ellipses

Table 1: Survey location.

Station ID	Location		Velocity [mm/yr]		Error [mm/yr]		Survey Date		Covariance
	Longitude	Latitude	East	North	East	North	Initial	Final	North/East
DEEP	-118.047197340	37.342553351	-6.0	4.8	0.3	0.4	2005.580822	2011.443836	-0.202
DYER	-118.039335035	37.742804198	-4.5	3.4	0.1	0.1	1999.580822	2010.745205	0.157
EPAS	-117.880704441	37.919669546	-4.0	2.2	0.3	0.4	2005.915068	2011.443836	0.494
FISH	-118.046284944	37.736988802	-3.9	3.5	0.3	0.2	1998.706849	2011.400000	0.169
FSH2	-118.006493295	37.567050615	-4.3	4.0	0.3	0.4	2005.413699	2011.443836	0.172
WOLF	-117.882875387	37.608271190	-4.7	2.9	0.2	0.3	2005.413699	2011.443836	-0.223
WSTG	-118.152016617	37.270726123	-6.0	4.9	0.2	0.3	1997.534247	2010.400000	0.219
WYMN	-118.001110266	37.412450141	-5.2	4.2	0.2	0.2	1998.734247	2010.380822	-0.054
P652	-118.238451253	37.589158034	-4.8	4.7	0.3	0.3	2007.915068	2011.695890	0.063

3.2 Displacement Model

Displacement rates for each survey location represent a velocity field for the study area around FLV and are displayed as resolved velocity vectors (Figure 4). Sites were selected to represent a near orthogonal transect across the fault plane. Model results are displayed in Figure 5. The solid black line represents the best fit solution for a far field velocity and locking depth across the FLV fault determined using a model grid search to determine the reduced-Chi square solution neatest 1.0. Shown is the fault parallel component of the observed velocities for each survey location with one sigma error bars, the only component of importance for the model. The survey locations are indicated by the normal distance from the fault plane. A reduced Chi square value of 2.004 represents the best fit curve. This value is above 1.0 and thus indicates the data set is not well fit to the curve. This result is expected as three of the nine measured velocities, DEEP, FISH, and P652, do not interest the predicted velocity The intersection of the predicted velocity and the fault plane is a floating arbitrary total velocity of ~5.8 mm/yr representing the regional displacement relative to the stable North America craton, presumably starting east of the Rocky Mountains. A displacement of ~3.8 mm/yr is observed between WSTG and EPAS, the farthest survey locations from the fault.

The reduced-Chi Square solutions for the far field velocity and locking depth grid search are represented in a contour profile (Figure 6). A well-bounded error well is not observed in the solution. The solutions were inspected in a three dimensional analysis and no local minima is observed in the values. The 65% and 95% confidence intervals are displayed in red and blue, respectively. While a defined range of locking depths can be determined for a small assumed total velocity, at larger velocities, the maximum locking

depths are unconstrained due to the limited spatial extent of the data and limitations in the occurrence of long-range elasticity, i.e. other faults exist, of the prescribed model. The far field velocities in the model span a range of ~60 km, but they are experiencing an additional elastic dislocation signal due to the location of nearby faults in the region. This effect increases the uncertainty of the predicted velocity and does not allow the calculation of an error interval for the modeled slip rate across the FLV fault. The ~3.8 mm/yr displacement determined in the model results does intersect the 65% confidence interval at a locking depth of 10-22 km which represents an acceptable solution for the region but is not constrained by the results.

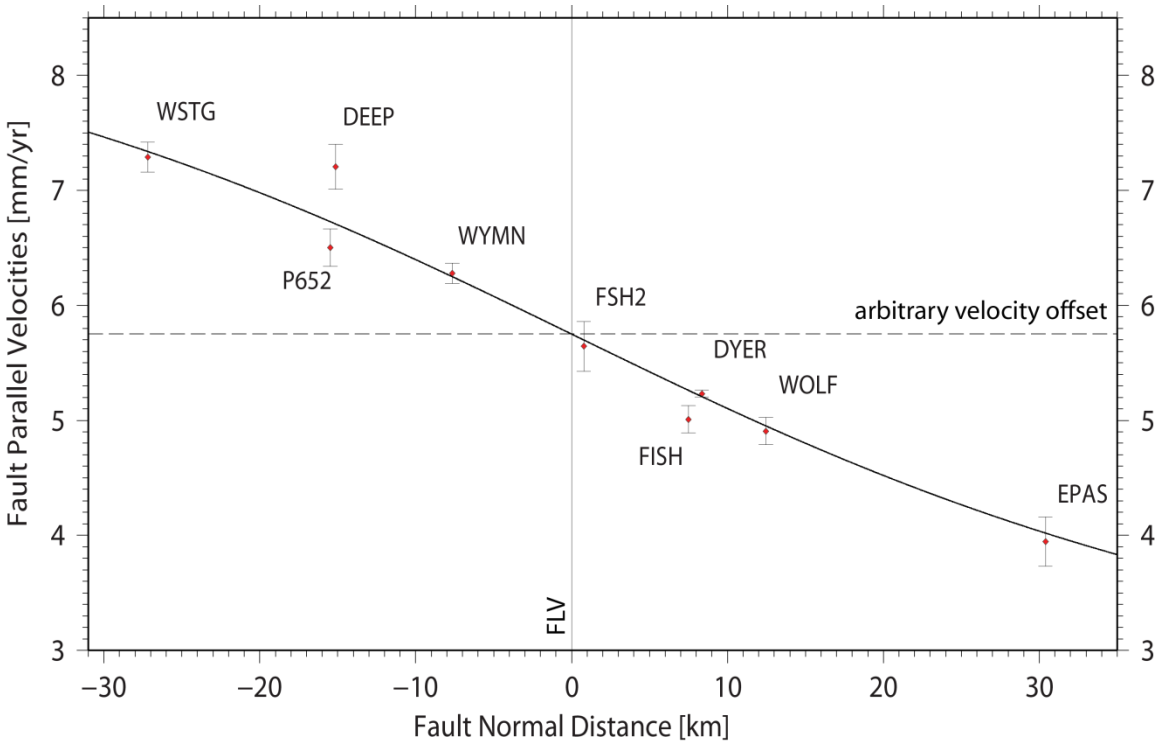

Figure 5: Shown are the observed velocities with one sigma error and the normal distance to the fault plane. The solid line is the best fit solution from a model grid search that allows for a floating arbitrary total velocity. The velocities displayed are the fault parallel component, the only component of importance for the assumed model.

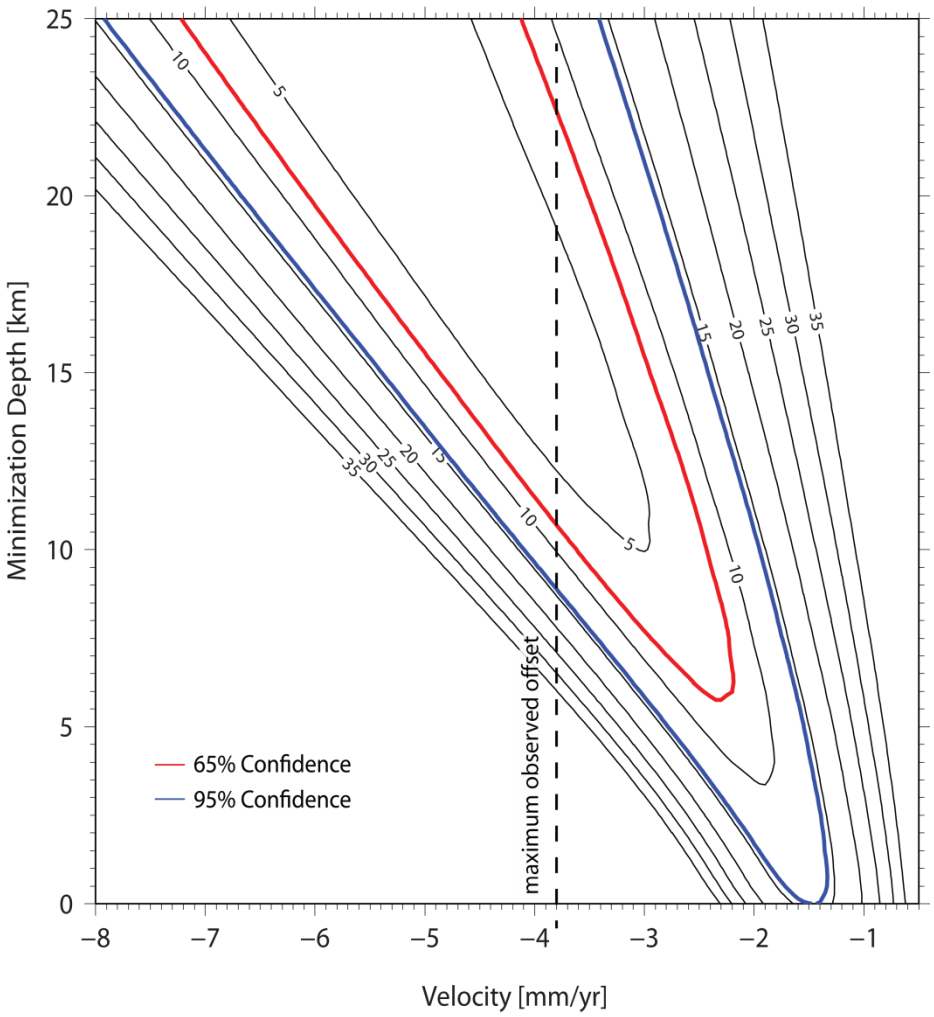

Figure 6: Reduced-Chi Square error.

CHAPTER 4

DISCUSSION

The aim of this study is to examine the strain accumulation on the FLV fault, a subsidiary fault of the Pacific-North American plate boundary located in the ECSZ, in particular to investigate if constancy exists in strain rates from the late Pleistocene through the Holocene. Structurally the FLV fault is a significant component in the eastward transfer of strain into the Mina Deflection and Basin and Range (Reheis and Sawyer, 1997) as well as accommodating rotational strain associated with the Sierra Nevada (Dixon et al., 2000). Quaternary slip rates indicate a slip rate of 6.1 +1.3/-1.0 mm/yr in the southern section of FLV at Cucomongo Canyon that decrease to 3.1 +0.5/-0.4 mm/yr at Furnace Creek and 2.2 +0.8/-0.6 at Indian Creek in northern FLV (Figure 1; Frankel et al., 2007; Frankel et al., 2011). This implies a transfer of strain east as the fault terminates in northern FLV and extensional faulting in the northern section of the valley.

Displacement model results from GPS measurements in this study indicate a slip rate of ~3.8 mm/yr on the central section of the FLV fault (Figure 5). This rate introduces questions for the surrounding structures in the region. The regional dextral transtensional shear rate of 9.3 ± 0.3 mm/yr represents ~25% of the total plate boundary motion in the study area and the strain must be accommodated on structures at ~37.5º N (Bennet et al, 2003). The 8.2±2.0 mm/yr (Dixon et al., 2000) displacement predicted is not observed and suggests validity for unexpressed structures accumulating strain in the region. The displacement observed in this study does correspond to the suggested eastward transfer of strain off the FLV fault beginning at Leidy Creek (Reheis and Sawyer, 1997; Ganev et

al., 2010; Foy, 2011; Frankel et al., 2011). Studies concerning the extensional rates east of the FLV fault represent <2 mm/yr and do not represent the total strain budget (Ganev et al., 2010; Hoeft et al., 2010; Foy, 2011). This would imply the rate of strain accumulation on the White Mountain fault is faster than the presumed 0.3-0.4 mm/yr geologic rate determined for the late Pleistocene (Kirby et al., 2006) and the modern slip rate on the Owens Valley fault would be closer to 7 mm/yr as reported by Dixon et al. (2000).

The determined rate on the FLV fault in this study is limited by the first order half space model design implemented on the data set. With nearby faulting and lacking an error interval, a true sense of strain transfer is not possible and questions remain on which structure or structures the total strain budget is dispersed. Additionally, the assumption is that the FLV fault is in the middle of the earthquake cycle, of unknown length, that results in an uninhibited interseismic signal along the fault. While results indicate a constancy in temporal strain accumulation a new model is needed that includes increasing the transect length across multiple faults to the east and west. The modeled velocity will remain a poor fit with a reduced Chi square value greater than one until all seismic activity is accounted for in the displacement signal.

CHAPTER 5

CONCLUSION

This study builds upon ongoing research to unravel the mystery of temporal and spatial of strain accumulation in regions of diffuse active faulting. The FLV fault is an active structure in the ECSZ with a history of temporal changes in strain accumulation and the most recent rupture date still unknown. A GPS campaign resulted in a near orthogonal transect across the fault containing nine survey locations with a range of ~60 km. Modeling results indicate a poorly constrained slip rate of ~3.8 mm/yr on the FLV fault using a first order elastic half space dislocation method. Survey locations in the far field display effects of additional interseismic signals from adjacent faults in the region. This effect produces a best fit solution with a reduced Chi square value greater than one. Future research in the region should focus on incorporation of two or more modeling techniques. These improvements would help to constrain the effects of unknown structure in the study area and serve to validate the results.

CHAPTER 6

REFERENCES

Bennett, R. A., B. P. Wernicke, N. A. Niemi, A. M. Friedrich, and J. L. Davis (2003), Contemporary strain rates in the northern Basin and Range province from GPS data, *Tectonics*, *22*(2) doi:10.1029/2001tc001355.

Dixon, T. H., M. Miller, F. Farina, H. Z. Wang, and D. Johnson (2000), Present-day motion of the Sierra Nevada block and some tectonic implications for the Basin and Range province, North American Cordillera, *Tectonics*, *19*(1), 1-24, doi:10.1029/1998tc001088.

Dixon, T. H., E. Norabuena, and L. Hotaling (2003), Paleoseismology and Global Positioning System: Earthquake-cycle effects and geodetic versus geologic fault slip rates in the Eastern California shear zone, *Geology*, *31*(1), 55-58, doi:10.1130/0091-7613.

Foy, Travis A. (2011), Quaternary faulting in Clayton Valley, Nevada: implications for distributed deformation in the Eastern California shear zone-walker lane, 100 pp, Georgia Institute of Technology, Atlanta.

Frankel, K. L., J. F. Dolan, R. C. Finkel, L. A. Owen, and J. S. Hoeft (2007), Spatial variations in slip rate along the Death Valley-Fish Lake Valley fault system determined from LiDAR topographic data and cosmogenic Be-10 geochronology, *Geophysical Research Letters*, *34*(18) doi:10.1029/2007gl030549.

Frankel, K. L., J. F. Dolan, L. A. Owen, P. Ganev, and R. C. Finkel (2011), Spatial and temporal constancy of seismic strain release along an evolving segment of the Pacific-North America plate boundary, *Earth and Planetary Science Letters*, *304*(3-4), 565-576, doi:10.1016/j.epsl.2011.02.034.

Friedrich, A. M., B. P. Wernicke, N. A. Niemi, R. A. Bennett, and J. L. Davis (2003), Comparison of geodetic and geologic data from the Wasatch region, Utah, and implications for the spectral character of Earth deformation at periods of 10 to 10 million years, *Journal of Geophysical Research-Solid Earth*, *108*(B4) doi:10.1029/2001jb000682.

Ganev, P. N., J. F. Dolan, K. L. Frankel, and R. C. Finkel (2010), Rates of extension along the Fish Lake Valley fault and transtensional deformation in the Eastern California shear zone-Walker Lane belt, *Lithosphere*, *2*(1), 33-49, doi:10.1130/l51.1.

Hammond, W. C., and W. Thatcher (2007), Crustal deformation across the Sierra Nevada, northern Walker Lane, Basin and Range transition, western United States measured with GPS, 2000-2004, *Journal of Geophysical Research-Solid Earth*, *112*(B5) doi:10.1029/2006jb004625.

Hoeft, J. S., and K. L. Frankel (2010), Temporal variations in extension rate on the Lone Mountain fault and strain distribution in the eastern California shear zone-Walker Lane, *Geosphere*, *6*(6), 917-936, doi:10.1130/ges00603.1.

Lee, J., J. Garwood, D. F. Stockli, and J. Gosse (2009), Quaternary faulting in Queen Valley, California-Nevada: Implications for kinematics of fault-slip transfer in the eastern California shear zone-Walker Lane belt, *Geological Society of America Bulletin*, *121*(3-4), 599-614, doi:10.1130/b26352.1.

Lee, J., C. M. Rubin, and A. Calvert (2001), Quaternary faulting history along the Deep Springs fault, California, *Geological Society of America Bulletin*, *113*(7), 855-869, doi:10.1130/0016-7606(2001)113<0855:qfhatd>2.0.co;2.

Kirby, E., D. W. Burbank, M. Reheis, and F. Phillips (2006), Temporal variations in slip rate of the White Mountain Fault Zone, Eastern California, *Earth and Planetary Science Letters*, *248*(1-2), 168-185, doi:10.1016/j.epsl.2006.05.026.

Malservisi, R., K. P. Furlong, and T. H. Dixon (2001), Influence of the earthquake cycle and lithospheric rheology on the dynamics of the Eastern California shear zone, *Geophysical Research Letters*, *28*(14), 2731-2734, doi:10.1029/2001gl013311.

Oldow, J. S. (2003), Active transtensional boundary zone between the western Great Basin and Sierra Nevada block, western US cordillera, *Geology*, *31*(12), 1033-1036, doi:10.1130/g19838.1.

Oskin, M., L. Perg, D. Blumentritt, S. Mukhopadhyay, and A. Iriondo (2007), Slip rate of the Calico fault: Implications for geologic versus geodetic rate discrepancy in the Eastern California Shear Zone, *Journal of Geophysical Research-Solid Earth*, *112*(B3) doi:10.1029/2006jb004451.

Reheis, C., and T. L. Sawyer (1997), Late Cenozoic history and slip rates of the Fish Lake Valley, Emigrant Peak, and Deep Springs fault zones, Nevada and California, *Geological Society of America Bulletin*, *109*(3), 280-299, doi:

Savage, J. C., and R. O. Burford (1973), Geodetic determination of relative plate motion in central California, *Journal of Geophysical Research*, *78*(5), 832-845, doi:10.1029/JB078i005p00832.

Wesnousky, S. G. (2005a), Active faulting in the Walker Lane, *Tectonics*, *24*(3) doi:10.1029/2004tc001645.

Wesnousky, S. G. (2005b), The San Andreas and Walker Lane fault systems, western North America: transpression, transtension, cumulative slip and the structural evolution of a major transform plate boundary, *Journal of Structural Geology*, *27*(8), 1505-1512, doi:10.1016/j.jsg.2005.01.015.